Chaotic consumption patterns in a simple 2-D addiction model.

Feichtinger, G.; Hommes, C.H.; Milik, A.

DOI
10.1007/s001990050151
Publication date
1997

Published in
Economic Theory

Economic Theory 10, 147–173 (1997)

Economic Theory

Chaotic consumption patterns in a simple 2-D addiction model*

Gustav Feichtinger[1], Cars Hommes[2], and Alexandra Milik[1]

[1] Institute for Econometrics, Operations Research and System Theory, University of Technology, A-1040 Vienna, AUSTRIA

[2] Department of Economic Statistics and Tinbergen Institute, University of Amsterdam, 1018 WB Amsterdam, THE NETHERLANDS

Received: April 4, 1994; revised version March 25, 1996

Summary. Consumption fluctuations in a simple 2-D addiction model are investigated. The behavioural equations of the model are suggested by a related 'rational addiction' model of Becker and Murphy [2]. Our model generates erratic, seemingly unpredictable consumption patterns of the addicted persons. The occurence of chaos is proven by locating a so called horseshoe map in the phase space.

JEL Classification Numbers: E32, D11, C60.

1 Introduction

There is a growing literature assuming that current consumption is affected by past consumption. A good review is provided by Becker in [1] who was one of the pioneers in intertemporal consumption dependencies (see e.g. [31]). Becker [1] cites Hicks [15] who critizises the independence assumption as follows:

"*It is nonsense that succesive consumptions are independent; the normal condition is that there is a strong complementarity between them.*"

Other early contributions on intertemporally dependent preferences include Wan [34], Samuelson [27], Spitzer and Wan [30] and Majumdar [21]. Following earlier work on the formation of consumption habits (see e.g.

* This work has been financially supported by the Austrian Science Foundation, project No. 7783-PHY. Part of the paper was written during a visit of one of the authors (CH) to the Institute for Econometrics, Operations Research and Systems Theory, University of Technology, Vienna. The kind hospitality during this visit is gratefully acknowledged. We thank an anonymous referee and the editor Prof. C.D. Aliprantis for helpful comments on an earlier draft of the paper leading to several improvements.

[26]) Becker and Murphy [2] define habitual behaviour as displaying a positive relation between past and current consumption. They present a model of *cycles* or *binges* in the amount of eating that has both short-term substitutions and long-term complementarities over time in food consumption.

Becker and Murphy [2] analyse a 'rational addiction' model, in which consumer behaviour of addicted persons is the result of intertemporal utility maximization. They identify conditions for a rational consumer to develop a habit; see also [26, 17, 18]. A necessary condition for habitual behaviour is that greater past consumption raises the marginal utility from present consumption. Moreover, the larger the discount rate on future utilities, the more likely a good is habitual. Furthermore, the depreciation rates play an important role for the development of a habit.

Becker [1] defines an *addiction* simply as a strong habit. In [8] Dockner and Feichtinger derive conditions being sufficient for an endogenously generated *persistent* cyclical consumption path. Using the Hopf bifurcation theorem they show that under certain assumptions stable limit cycles are compatible with rational (i.e. intertemporally maximizing utility) behaviour. As Becker and Murphy [2] carry out, a habit becomes an addiction when the effects of past consumption on present consumption are sufficiently strongly *destabilizing*.

Considering periodic patterns as a first step to the route to chaotic behaviour it seems to be quite natural to ask whether more complex consumption patterns than persistent cycles can occur. It is well-known that there exist several types of heavy drinkers. One of them, the so-called gamma-drinkers go on binges, i.e. they show more or less periodic ups and downs of consumption of alcohol. The model we present below exhibits even more irregular, random looking consumption patterns.

The purpose of the present paper is to identify conditions generating chaotic consumption paths. A first step in that direction has already been made by Feichtinger in [10] (see also [9] and [12]). To study the question we consider a discrete-time framework. In particular, a discrete time version of the state equations in [8] is used. The consumption rate however is determined by a feedback rule which is suggested by the dynamic optimization framework of Becker and Murphy [2] (for details see section 2). The main result for our discrete time model is that in addition to stable cycles, chaotic, seemingly unpredictable consumption fluctuations can occur.

The addiction model is a 2-D discrete time system. The present paper serves an important second, methodological purpose, namely describing a method of proving the occurrence of chaos in a 2-D system. In the literature, in most examples of economic models exhibiting chaos, the dynamical behaviour is described by or reduced to a 1-D difference equation.[1] Concerning the few 2- or higher dimensional examples that have appeared in

[1] For a survey and examples of 'chaos in economics' see e.g. [20, 5, 16, 22, 6].

the economic literature, the occurrence of chaos is mainly shown by numerical simulation.

For 1-D systems the occurrence of (topological) chaos is relatively easy to show, by investigating the graph of the associated 1-D map and e.g. by using the well-known 'Period three implies chaos' theorem by Li and Yorke [19]. In a 2-D system however, it is much more difficult to prove the occurrence of (topological) chaos. Our numerical results indicate the occurrence of strange, chaotic attractors in the 2-D addiction model. By applying the well-known 'horseshoe-theorem' by Smale [28] we are able to establish the occurrence of (topological) chaos rigourously[2]. The method is mainly geometric and relies on locating a suitable rectangular region in the phase space, which is mapped over itself in the form of a 'horseshoe'.

Existence of horseshoes need not imply chaotic dynamical behaviour in the long run however. In the presence of a horseshoe chaos may be a transient phenomenon and Lebesgue almost all initial states may still converge to e.g. a stable steady state. Very recently, two closely related papers by de Vilder [32,33] and Brock and Hommes [4][3], concerning existence of chaos and strange attractors in 2-D discrete economic models have appeared, applying recent mathematical results on homoclinic bifurcations and its associated complicated dynamics (for an excellent mathematical survey see Palis and Takens [25]). We briefly discuss how these results can be applied to prove the existence of strange attractors for a large set of parameter vaules in the 2-D addiction model.

The paper is organized as follows. Section 2 describes the model, while section 3 contains some numerical simulations. The main contribution of the paper is section 4, analyzing the global dynamics of the model. Finally, section 5 contains some concluding remarks and the proofs of the results are given in an appendix.

2 The model

The model describes a single consumption good c_t accumulating two distinct stocks of consumption capial s_t and w_t. More specifically consider e.g. the overeating-dieting problem. Here s_t denotes the eating capital (habit) and w_t the health status (weight) of the consumer. The stocks accumulate by consumption and decumulate with constant depreciation rates δ and α. In discrete time these assumptions yield the equations

$$s_{t+1} = (1-\delta)s_t + c_t \quad 0 < \delta < 1 \tag{1}$$

$$w_{t+1} = (1-\alpha)w_t + c_t \quad 0 < \alpha < 1 \tag{2}$$

[2] Sorger [29] proved the occurrence of topological chaos in a 2-D discrete time infinite horizon economy, by showing the existence of a so-called "snap-back repeller".

[3] Both papers [32, 33] and [4] have been written after submission of the first draft of the present paper.

where consumption $c_t = c(s_t, w_t)$ depends on the two stock variables s and w.

Concerning the consumption *feedback rule* $c(s, w)$ we make the general assumptions that $\frac{\partial c}{\partial s} > 0$ while $\frac{\partial c}{\partial w} < 0$. Hence, consumption becomes larger when the habit s increases ('addiction') but consumption becomes smaller when the weight w increases.

Since our aim is to investigate the global dynamical behaviour of the model, we have to specify a consumption feedback rule satisfying these assumptions. We choose

$$c_t = c(s_t, w_t) = \frac{s_t^{\beta}}{(w_t - w_{min})^{\gamma}} \quad 0 < \beta < 1,\ \gamma > 1 \quad \text{and } w_{min} \geq 0 \qquad (3)$$

and note that other feedback rules satisfying $\frac{\partial c}{\partial s} > 0$ and $\frac{\partial c}{\partial w} < 0$ yielded similar results. The parameters β and γ measure the consumption elasticity w.r.t. the habit s and the weight w respectively; w_{min} denotes some nonnegative natural minimal weight[4].

The feedback rule for consumption may be justified as follows. As Dockner and Feichtinger show in [8], the *optimal* consumption rate is by linearisation around the steady state a linear function of both state variables s_t, w_t. In addition, the discussion in [2] shows that addiction (in the sense sketched in the introduction) implies that consumption c is *positively* correlated with s, and *negatively* correlated with w. The arguments are summarized in [8, p. 259, 260]. The addictive force causes current consumption to rise as past consumption accumulates while the satiating force causes it to fall. In [8] it is shown that the two counterbalancing forces may create cyclical consumption patterns. There is no reason to restrict ourselves to a *linear* feedback consumption rule. The assumption on second-order derivatives of $c(s, w)$ seem to be quite natural on economic terms. Both the habit and the health status are assumed to have a marginally decreasing effect on the consumption rate.

We emphasize that the model has a very simple and general structure. Two stock-variables decaying with constant depreciation rates α and δ and at the same time accumulating by a feedback rule depending on both stock variables. As the first stock variable increases, the feedback gets stronger, whereas the feedback gets weaker when the second stock-variable increases.

The model (1)–(3) is a 2-D difference equation $(s_{t+1}, w_{t+1}) = F(s_t, w_t)$, with

$$F(s, w) = \begin{pmatrix} (1-\delta)s + c(s, w) \\ (1-\alpha)w + c(s, w) \end{pmatrix} \quad \text{and} \quad c(s, w) = \frac{s^{\beta}}{(w - w_{min})^{\gamma}} \qquad (4)$$

Straightforward computation shows that the model has a unique steady state (s^{eq}, w^{eq}). In the general case $w_{min} > 0$ no analytic expression can be

[4] In all numerical and theoretical results below we restrict our attention to parameters for which the weight $w_t > w_{min}$ for all time t.

obtained, but in the case $w_{min} = 0$ the steady state is:

$$\begin{pmatrix} s^* \\ w^* \end{pmatrix} = \begin{pmatrix} \frac{\alpha}{\delta}\left(\frac{1}{\alpha}\left(\frac{\alpha}{\delta}\right)^{\beta}\right)^{1/(\gamma+1-\beta)} \\ \left(\frac{1}{\alpha}\left(\frac{\alpha}{\delta}\right)^{\beta}\right)^{1/(\gamma+1-\beta)} \end{pmatrix} \tag{5}$$

First we investigate the stability of the steady state. The Jacobian matrix of F is

$$JF(s,w) = \begin{bmatrix} 1-\delta+\frac{\partial c}{\partial s} & \frac{\partial c}{\partial w} \\ \frac{\partial c}{\partial s} & 1-\alpha+\frac{\partial c}{\partial w} \end{bmatrix} \tag{6}$$

and the corresponding characteristic equation for the eigenvalues is

$$\begin{aligned} \lambda^2 - \lambda\left(1-\delta+\frac{\partial c}{\partial s}+1-\alpha+\frac{\partial c}{\partial w}\right) + \left(1-\delta+\frac{\partial c}{\partial s}\right)\left(1-\alpha+\frac{\partial c}{\partial w}\right) \\ - \frac{\partial c}{\partial s}\frac{\partial c}{\partial w} = 0 \end{aligned} \tag{7}$$

With the consumption $c(s,w) = s^{\beta}/(w - w_{min})^{\gamma}$ and using the fact that $c(s^{eq}, w^{eq}) = \delta s^{eq} = \alpha w^{eq}$ we get

$$\frac{\partial c}{\partial s}(s^{eq}, w^{eq}) = \beta\delta \quad \text{and} \quad \frac{\partial c}{\partial w}(s^{eq}, w^{eq}) = -\alpha\gamma\frac{w^{eq}}{w^{eq} - w_{min}}.$$

The characteristic equation for the stability of the steady state than becomes

$$\begin{aligned} \lambda^2 - \lambda\left(1-\delta+\beta\delta+1-\alpha-\alpha\gamma\frac{w^{eq}}{w^{eq}-w_{min}}\right) \\ + (1-\delta+\beta\delta)\left(1-\alpha-\alpha\gamma\frac{w^{eq}}{w^{eq}-w_{min}}\right) + \alpha\beta\gamma\delta\frac{w^{eq}}{w^{eq}-w_{min}} = 0 \end{aligned} \tag{8}$$

A simple computation shows that when the eigenvalues are complex, the steady state is stable. Furthermore, when the eigenvalues are real, the largest eigenvalue is always smaller than 1. Therefore, the steady state can not lose stability via a Hopf-bifurcation (two complex eigenvalues crossing the unit circle) or via a saddle-node bifurcation (the largest real eigenvalue crossing $+1$), but it can only lose stability via a period-doubling bifurcation (the smallest real eigenvalue crossing -1). The condition that the smallest eigenvalue is -1 yields the following period-doubling bifurcation curve in the parameter space:

$$(1-\alpha)(2-\delta+\beta\delta) + (2-\delta)\left(1-\alpha\gamma\frac{w^{eq}}{w^{eq}-w_{min}}\right) + \beta\delta = 0 \tag{9}$$

To summarize, the steady state is stable when both eigenvalues are complex, or both eigenvalues are real and the LHS in (9) is positive. This is e.g. the case when α or γ are sufficiently close to 0. The steady state is unstable when both eigenvalues are real and the LHS in (9) is negative. This is e.g. the case when γ is sufficiently large. In the next sections we will investigate the

consumption patterns when the steady state is unstable. In particular we shall investigate what happens after the period doubling bifurcation.

3 Numerical simulations

In this section we investigate the habit, weight and consumption fluctuations by numerical simulations. We choose the parameters $\alpha = 0.1, \beta = 0.1, \gamma = 3$ and $\delta = 0.5$ as a benchmark case. In section 4 we will prove the occurrence of (topological) chaos for this and other choices of the parameters. This section is subdivided into two parts. First we examine some characteristic features of the attractors in the phase space and of the time series. Secondly we investigate the bifurcation scenario, i.e. we investigate how the habit, weight and consumption patterns change when one of the parameters is varied.

3.1 Strange attractors and chaotic time series

An attractor is a set of points representing the long term dynamical behaviour of the system. There are several definitions of attractors; for a discussion see Milnor [23]. A frequently used definition is:

Definition 1. *An attractor of a K-dimensional system $X_{t+1} = F(X_t)$ is a compact set A with the following properties:*

1. *The set A is invariant, i.e. $F(A) \subset A$.*
2. *There exists an open neighbourhood U of A, such that $F(U) \subset U$ and for each initial state $X_0 \in U, \lim_{n\to\infty} dist(F^n(X_0), A) = 0$.*
3. *There exists an initial state $X_0 \in A$ for which the orbit is dense in A.*

A set A satisfying only the first two properties is called an *attracting* set. The second property states that all initial states in some neighbourhood of A converge to the attractor. The third property ensures that A is the smallest set satisfying the first two properties.

The simplest example of an attractor is a stable equilibrium. Another simple example is a stable periodic orbit, in which case the attractor consists of only finitely many points. In nonlinear systems, however, much more complicated attractors consisting of infinitely many points with a complicated geometric structure may occur. These so called strange, chaotic attractors correspond to erratic, seemingly unpredictable dynamical behaviour of the system. Again there are several definitions for the notion of strange attractor. We use the following, see e.g. Palis and Takens [25] for a mathematical treatment.

Definition 2. *An attractor A is called a strange attractor, if:*

1. *A is the closure of the unstable manifold of some (periodic) saddle point.*
2. *There exists a point $X_0 \in A$ such that the orbit of X_0 is dense in A and has a positive Lyapunov exponent.*

A strange attractor has a fractal structure, since unstable manifolds may oscillate wildly, accumulating on itself. The second property implies that orbits converging to a strange attractor exhibit sensitive dependence on initial conditions.

Figure 1 presents phase-space plots of the attractors for different values of γ. Each picture shows a finite number of points (say 10000) of an orbit in the (s, w)-plane, after a short transient (the initial part of the orbit of say the first 10 points has been neglected). Figure 1a shows a stable period 4 orbit, while figures 1b–d indicate the occurrence of strange, chaotic attractors. Figures 1e–f are enlargements of 1c, suggesting a fractal, Cantor-like structure of the attractors. Furthermore notice that the strange attractors in figures 1b–d have two, three and four 'branches' respectively.

Figures 1g–h show attractors for different values of δ. The attractors seem to be qualitatively the same as before, but as δ gets closer to $\alpha = 0.1$,

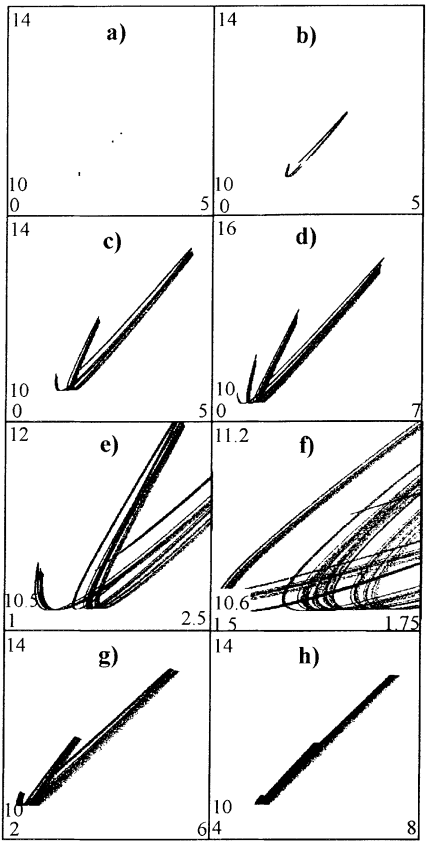

Figure 1a–b. Attractors in the (s, w) phase space, with $\alpha = 0.1, \beta = 0.1$ and $w_{min} = 10$. **a–e** $\delta = 0.5$: (a) $\gamma = 2.25$: a stable period 4 orbit, **b–d** strange, chaotic attractors for $\gamma = 2.5$, 3 and 3.5, **e–f** enlargement of the strange, chaotic attractor in (d). **g–h** $\gamma = 3$: (g) $\delta = 0.35$, (h) $\delta = 0.2$.

the strange attractor gets closer and closer to a line segment. In fact it is straightforward to show that, for $\delta = \alpha$, the 2-D addiction model reduces to a 1-D system. More precisely, for $\delta = \alpha$ the diagonal $s = w$ is an attracting set and the dynamics on this attracting set is described by the 1-D difference equation.

$$w_{t+1} = (1 - \delta)w_t + \frac{w_t^{\beta}}{(w_t - w_{min})^{\gamma}}$$

Although the proof of this statement is straightforward, we omit it since we want to focus on the 2-D case.

Figure 2 shows the chaotic habit, weight and consumption fluctuations corresponding to the strange attractor in figure 1c. Chaotic time paths are often characterized by a mixture between regular and irregular behaviour. The consumption time path in figure 2a is characterized by phases of 1, 2 or 3 consecutive periods where consumption is low, followed by a sudden burst

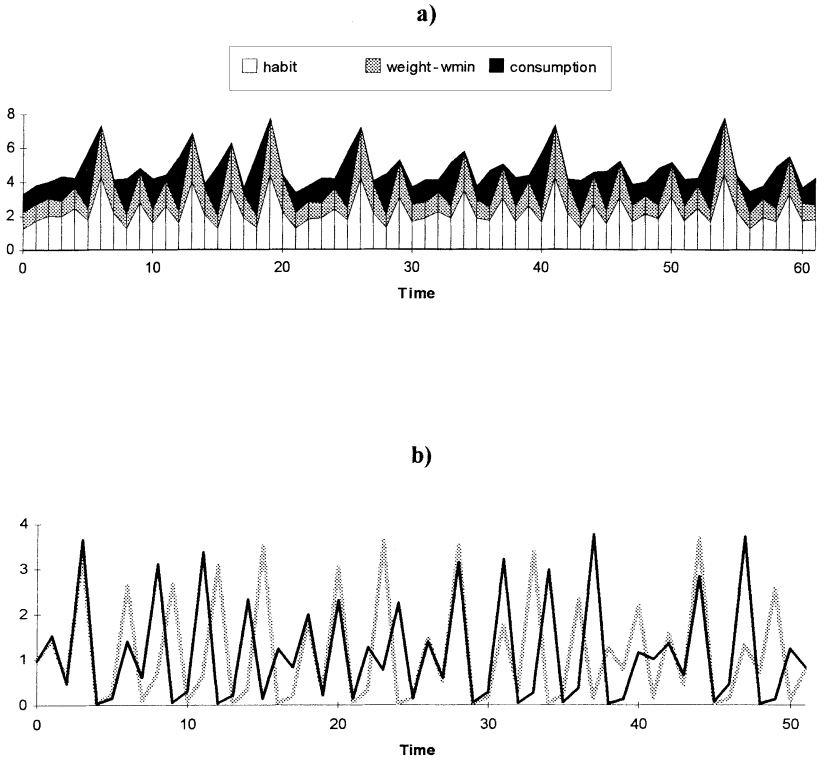

Figure 2a. Chaotic time series of the habit s, the weight w and the consumption c, corresponding to the strange attractor for $\alpha = 0.1, \beta = 0.1, \gamma = 3, \delta = 0.5$ and $w_{min} = 10$ in figure 1. **b** Two chaotic consumption time series with initial states $(s_0, w_0) = (1, 11)$ and $(s_0, w_0) = (1, 11.001)$ respectively, illustrating the sensitivity of the consumption patterns to the initial states.

of high consumption. The behaviour of the weight w seems to be qualitatively the same as the behaviour of the habit s. The periods in which the high consumption peaks occur seem to be difficult to predict and depend sensitively on the initial states (see figure 2b).

The numerical simulations indicate that when the parameter γ, measuring the elasticity of consumption w.r.t. weight, increases, the dynamical behaviour becomes more complicated. Apparently, a high value of γ can lead to irregular consumption patterns. An intuitive explanation of this observation is the following. For high γ, a weight w close to the minimum weight w_{min} leads to a high consumption. A high consumption leads to a high weight in the next period and a corresponding low consumption. As long as consumption is low, weight will decrease. This decrease continues for one or more consecutive periods, until the weight is low and gets close to its minimum value w_{min}, so that consumption becomes high again and the next 'cycle' starts. When γ is high, this nonlinear interaction between consumption and weight is strong and may cause erratic fluctuations.

3.2 Parameter dependence

In this subsection we investigate how the dynamical behaviour changes when one of the parameters is varied. Figure 3 shows bifurcation diagrams with the other parameters fixed as in the benchmark case, at $\alpha = 0.1, \beta = 0.1, \gamma = 3$ and $\delta = 0.5$.

Figure 3a shows the familiar period doubling bifurcation route to chaos, when α is increased from 0 to 0.14. The first period doubling bifurcation from a stable equilibrium to a stable period two orbit occurs for $\alpha \approx 0.07$. Apparantly, increasing the depreciation rate α of the weight w, makes the dynamical behaviour more complicated. An intuitive explanation of this observation is the following. Suppose that weight is high, so that the corresponding consumption will be low. For higher α-values weight will decrease more rapidly, until it is close to its minimum w_{min}. When weight is close to its minimum, the corresponding consumption will be high leading to a high weight in the next period again. Hence, for higher α-values large, possibly erratic fluctuations in both weight and consumption, and therefore also in habit, may occur.

The bifurcation diagram in figure 3b suggests the occurrence of chaotic behaviour for low values of β. Via a sequence of period halving bifurcations a stable 3-cycle for $\beta \approx 0.4$. In that case numerical experiments indicate that a typical time paths is characterized by an initial erratic part before settling down to the stable 3-cycle. For higher values of β a another sequence of period halfings leads to a period two cycle for values of β close to 1[5].

[5] Figure 3b suggests that higher β-values lead to regular behaviour. However, we note that even for the maximum β-value, $\beta = 1$, strange attractors can occur, e.g. for $\gamma = 3.5$ (i.e. when γ is larger than in our benchmark case). In particular, the primary period doubling bifurcation condition (9) shows that even for $\beta = 1$ the steady state can be strongly unstable when γ is high.

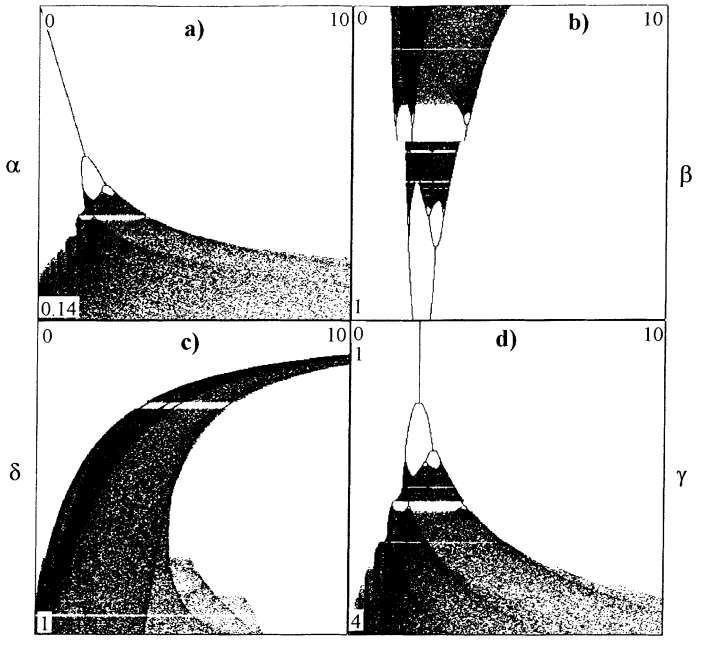

Figure 3. Bifurcation diagrams from the benchmark case $\alpha = 0.1, \beta = 0.1, \gamma = 3, \delta = 0.5$ and $w_{min} = 10$.

Figure 3c shows the bifurcation diagram w.r.t. the depreciation rate of the habit s, i.e. the parameter δ. For most values of δ the dynamical behaviour seems to be chaotic. It seems that the qualitative dynamical behaviour is not very sensitive to the parameter δ.

Finally, figure 3d shows the bifurcation scenario for γ between 1 and 4. The diagram confirms what we already observed in the subsection 3.1, namely that increasing γ leads to more complicated dynamical behaviour. For high values of γ the strong nonlinear interaction between weight and consumption produces erratic fluctuations.

We conclude that the qualitative dynamical behaviour of the model is very sensitive to the parameters α, β and γ, while it is much less sensitive to the parameter δ. In particular, the numerical results indicate that a high value of γ leads to erratic consumption patterns. A strong nonlinear interaction between weight and consumption seems to be responsible for the erratic fluctuations. This numerical observation will be confirmed by the theoretical results in the next section.

4 Global dynamics

The addiction model is a 2-D difference equation $(s_{t+1}, w_{t+1}) = F(s_t, w_t)$. The numerical results in section 3 suggest the occurrence of strange, chaotic attractors for many parameter values. However, to prove the existence of

strange, chaotic attractors is a nontrivial task. In this section we present theoretical results concerning the complexity of the global dynamical behaviour. The section is subdivided into three subsections. In the first we briefly recall Smale's classical horseshoe, while in the second we present results concerning the existence of horseshoes in the addiction model, implying topological or transient chaotic phenomena. In the third subsection we discuss very recent mathematical results concerning existence of strange attractors in 2-D models like our addiction model.

4.1 Smale's horseshoe

For 1-D systems the easiest way to prove the occurrence of topological chaos is by showing the existence of a period three orbit and use the "Period three implies chaos" result by Li and Yorke [19]. Since this result only holds for continuous 1-D systems, it can not be applied to the present 2-D model. In a 2- or higher dimensional system there is however a different method to show the existence of topological chaos, namely via the existence of so-called horseshoes.

In this subsection, we briefly recall the essential features of the classical horseshoe-map due to Smale [28]; for additional details see e.g. textbook treatments in [7] or [13]. Consider a rectangular region $R = \overline{A_0 B_0 C_0 D_0}$ together with two semi-disks S and T, as in figure 4a. Let $D = S \cup R \cup T$ and define a map G on D with the following properties. The map G shrinks D horizontally by a factor $< 1/3$, expands D vertically by a factor 3 and folds the resulting figure so that it fits into D again. Hence $G(D)$ is contained in D and $G(D)$ has the form of horseshoe. The images of the points A_0, B_0, C_0 and D_0 are A_1, B_1, C_1 and D_1, and the images of the semi-disks S and T are small semi-disks contained in S. Furthermore there are two horizontal strips H_0 and H_1 in R which are mapped 1-1 into the vertical strips $V_0 = G(H_0)$

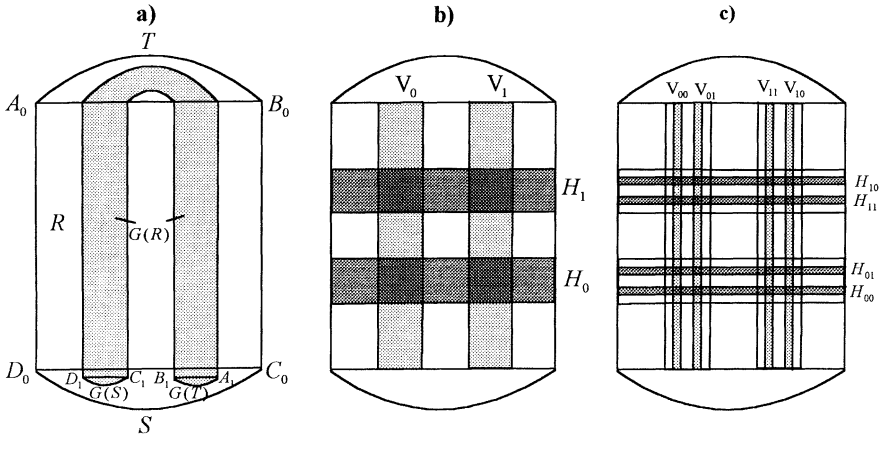

Figure 4. Smales's horseshoe-map.

and $V_1 = G(H_1)$ in R; for illustration see figure 4b. The subregion in R between H_0 and H_1 is mapped into the semi-disk T, while the subregions in R below H_0 and above H_1 are mapped into the semi-disks S.

What is the *maximal invariant set* Λ in R, that is, what is the set of points remaining in the region R for ever? The horizontal strips H_0 and H_1 are exactly those points $X \in R$ for which $G(X) \in R$. Each horizontal strip $H_i, i = 0, 1$, contains two smaller horizontal strips consisting of points X for which $G^k(X) \in R, k = 0, 1$ or 2, with $G^2(H_{00}) = G^2(H_{10}) \subset V_0$ and $G^2(H_{01}) = G^2(H_{11}) \subset V_1$, as in figure 4c. There are thus 4 horizontal strips $H_{ij}, i, j = 0, 1$, of points X for which $G^k(X) \in R$ for $k = 0, 1$ or 2. Continuing in the same way, it can be shown that there are 2^n disjoint horizontal strips consisting of points X for which $G^k(X) \in R$ for $0 \leq k \leq n$. Using the fact that the map G is expanding in the vertical direction, it can be shown that the *forward invariant set* L^+, that is the set of points $X \in R$ for which $G^n(X) \in R$, for all $n \in \mathcal{N}$, is a (zero Lebesgue measure) Cantor set of horizontal line segments. In the same way, it can be shown that the *backward invariant set* L^-, that is, the set of points X for which $G^{-n}(X) \in R$ for all $n \in \mathcal{N}$, is a (zero Lebesgue measure) Cantor set of vertical line segments. The maximal invariant set in R, i.e. the set of points that remain in R for both positive and negative time, is then given by $\Lambda = L^+ \cap L^-$. The maximal invariant set is thus an intersection of Cantor sets of vertical and horizontal line segments.

According to the classical result by Smale the dynamics of the map G on the invariant Cantor-set Λ is topologically equivalent to the shift automorphism on bi-infinite sequences of two symbols. For details see [28] or textbook treatments in e.g. [7] or [13]. The proofs in the appendix contain a discussion of the (symbolic) dynamics on a maximal invariant set in some rectangular region in the 2-D phase space of the addiction model. From the properties of the shift map on bi-infinite symbolic sequences of two symbols, it follows that the map G is topologically chaotic. More precisely, the dynamics on the invariant Cantor set Λ has the following properties:

1. Λ contains infinitely many unstable periodic points with different period.
2. Λ contains an uncountable set of aperiodic points (i.e. points whose orbits are not periodic and do not converge to a periodic orbit).
3. the map G has *sensitive dependence on initial conditions* in Λ, that is, there exists a $D > 0$ (the distance between the horizontal strips H_0 and H_1), such that for all $\bar{x}_0 \in \Lambda$ and each neighbourhood U of $\bar{x}_0$, there exists an $\bar{y}_0 \in \Lambda$, $\bar{x}_0 \neq \bar{y}_0$, and a time $N > 0$, such that $|G^N(\bar{x}_0) - G^N(\bar{y}_0)| > D$.

We will call such a set Λ **a chaotic invariant set** and say that the map G has a horseshoe.

It is important to note that despite the fact that the dynamical behaviour on the Cantor set Λ is complicated, for most initial states in its domain D the long term behaviour under the map G is regular. In fact G has a stable fixed point in the semi-disk S and Lebesgue almost all points converge to this

stable fixed point. The points which do not converge to the stable fixed point are precisely the points in the invariant Cantor set Λ, but this Cantor set has Lebesgue measure zero. The chaotic invariant set is thus not an attractor; Lebesgue almost all intial states eventually escape from the region R. This situation is usually referred to as *topological chaos*. The initial part of many orbits may be erratic, but eventually most orbits settle down to a stable steady state or a stable cycle. However, initial states close to the invariant Cantor set will mimic the chaotic dynamics for a long time before settling down to the stable fixed point. Therefore, from an economic point of view topological chaos is important, since the first say 100 points of a time path seem to be more relevant than that part of an orbit after a long transient.

In a two (or higher) dimensional discrete time model $X_{n+1} = F(X_n)$, existence of a horseshoe for the map F (or for some iterate F^k of F) is a sufficient condition for topological chaos. In a model exhibiting topological chaos, existence of strange chaotic attractors can be expected, possibly for a large set of parameter values (cf. the discussion in subsection 4.3). Proving topological chaos in a model is therefore an important first step.

4.2 Horseshoes in the 2-D addiction model

We present two theorems concerning the existence of horseshoes in the addiction model. We focus on the parameter γ and show that a horseshoe exists when γ is high. Proofs are given in the appendix. We emphasize that, much in the spirit of Smale and others in the field of nonlinear dynamical systems theory, the proofs are geometric rather than analytic. The main geometric arguments are sketched in this subsection.

The first theorem states that a horseshoe occurs when $\beta = 0$ and γ is large[6].

Theorem 1. *Assume that* $\beta = 0, \alpha = 0.1, \delta = \delta_0$ *and* $w_{min} = 10$ *are fixed.*

1. *For* $\gamma = 0.25$ *the map F has a globally stable steady state.*
2. *For* $\gamma \in [2.75, 50]$ *F is topologically chaotic and in particular, the third iterate* F^3 *has a horseshoe.*

Notice that, for $\beta = 0$, consumption $c(s, w) = 1/(w - w_{min})^{\gamma}$ only depends on the weight w. Hence, for $\beta = 0$, consumption is given by a negative feedback rule depending upon the weight. The dynamics is then described by

$$s_{t+1} = (1 - \delta)s_t + \frac{1}{(w_t - w_{min})^{\gamma}} \tag{10}$$

$$w_{t+1} = (1 - \alpha)w_t + \frac{1}{(w_t - w_{min})^{\gamma}} = f(w_t) \tag{11}$$

[6] For other values of the parameters α, β, δ and w_{min} than those in theorems 1 and 2, similar results can be obtained.

Hence, the dynamics of w is, independently of s, described by a one-dimensional difference equation. For γ large, the 1-D dynamics of w is chaotic, and therefore also the 2-D system (10–11) becomes chaotic. The assumption $\partial c/\partial w < 0$, i.e. the negative feedback of weight upon consumption, is in fact responsible for the erratic consumption patterns of habit, weight and consumption. Chaos occurs when the parameter γ measuring the consumption elasticity w.r.t. the weight w is large.

The horseshoe that arises in the 2-D model for the third iterate F^3 is illustrated in figure 5. Notice that the geometry of the horseshoe is different from Smale's classical example. The map F contracts the region R horizontally, stretches it vertically and folds it back along some segment P_0Q_0 to get the horseshoe like region $F(R)$ (figure 5b). This horeseshoe is then turned upside down, stretched vertically, contracted horizontally so that $F^2(R)$ is as in figure 5c. Finally, it is contracted both horizontally and vertically, so that $F^3(R)$ has the form of a horseshoe folded over R as in figure 5d.[7]

Although $\beta = 0$ is a special parameter value, where there is no positive feedback from the habit s upon consumption, we will see that this case captures the essential geometric features explaining the existence of horseshoes for the 2-D model with additional positive feedback, i.e. $\beta > 0$, as well. Now turn to the bench-mark case with the parameters $\alpha = 0.1, \beta = 0.1, \gamma = 3$ and $\delta = 0.5$. Define a *rectangular region* $\overline{ABCD}$ as the convex hull of the points A, B, C and D. We have:

Theorem 2. *For* $\alpha = 0.1, \beta = 0.1, \gamma = 3, w_{min} = 10$ *and* $\delta = 0.5$ *or* $\delta = 0.2$ *the map F is topologically chaotic. In particular:*

1. *For* $\delta = 0.5$ *the rectangular region* $R_1 = \overline{ABCD}$, *with* $A = (3.8, 13)$, $B = (4.3, 13)$, $C = (3.4, 12.1)$ *and* $D = (2.9, 12.1)$ *contains a chaotic invariant set.*
2. *For* $\delta = 0.2$ *the rectangular region* $R_2 = \overline{ABCD}$, *with* $A = (7, 13)$, $B = (8, 13)$, $C = (7, 12.2)$ *and* $D = (6, 12.2)$ *contains a chaotic invariant set.*

Figure 6 presents the geometric idea behind the proof. In figure 6a the rectangular region R_1 and the corresponding strange, chaotic attractor are shown. Notice that R_1 encloses the largest 'branch' of the strange attractor. Figure 6b shows the rectangular region R_1 together with its three images $F(R_1), F^2(R_1)$ and $F^3(R_1)$. $F^3(R_1)$ is folded as a horseshoe over R_1. The

[7] There are thus essentially two differences with Smale's classical horseshoe. In the present example the eigenvalue corresponding to the unstable direction is negative. This negative eigenvalue is caused by the transition from $F(R)$ to $F^2(R)$, since $F(R)$ is stretched and turned 'upside down'. The second difference is that, unlike Smale's horseshoe map, the map F is not a diffeomorphism on its entire domain. Especially, in the rectangular region $U_0V_0X_0W_0$ there exist pairs of points having the same image. Despite these differences, in a similar way as for Smale's horseshoe, the dynamics on the invariant set can be related to the shift map on bi-infinite sequences of two symbols; see the appendix.

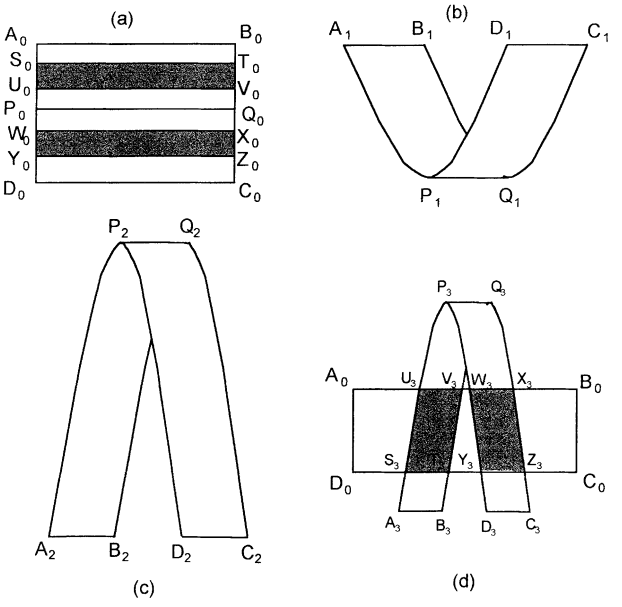

Figure 5. Schematic drawings of the first three iterates of the rectangular region R. The third iterate F^3 maps the rectangular region $R = \overline{A_0B_0C_0D_0}$ in the form of a horseshoe over itself, with contraction in the horizontal direction, stretching in the vertical direction and folding along the segment P_0Q_0.

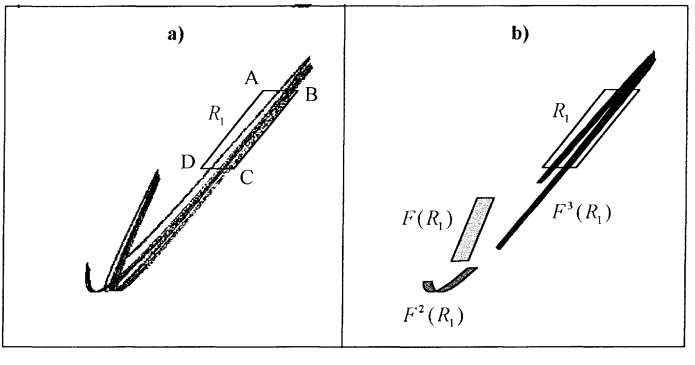

Figure 6a,b. $\alpha = 0.1, \beta = 0.1, \gamma = 3, \delta = 0.5$ and $w_{min} = 10$. **a** The strange, chaotic attractor and the rectangular regions R_1, **b** The chaotic region R_1 and its first three images $F(R_1), F^2(R_1)$ and $F^3(R_1)$.

main difference with the second region R_2 is that in the latter case, the two "vertical strips" of the horseshoe overlap. Nevertheless, R_2 does contain a chaotic invariant region.

Figure 6b nicely illustrate the three characteristic features of chaotic behaviour: contraction in one direction, stretching in another direction and folding. The (strong) contraction occurs in the s-direction and the stretching in the direction of the diagonal. The region $F(R_1)$ is a contraction of R_1 in

both the s- and w-direction, $F^2(R_1)$ is obtained from $F(R_1)$ by a contraction in the s-direction together with a folding and finally $F^3(R_1)$ is obtained from $F^2(R_1)$ by contraction in the s-direction and (strong) expansion along the diagonal direction.

Theorem 2 states that, for one particular choice of the parameters the dynamics of the model is topologically chaotic. In the proof of the theorem, it is important that the consumption level curves $c(s, w) = k$ are flat and close to horizontal lines when s in not close to 0; see the appendix for details. With consumption given by $c(s, w) = \dfrac{s^\beta}{(w - w_{min})^\gamma}$ this will be the case when γ is large. Therefore, we expect that (topological) chaos will occur whenever γ is large.

4.3 Strange attractors in the 2-D addiction model

In the previous subsection we have shown the existence of horseshoes in the 2-D addiction model. This implies topological chaos, but as noted before, when a horseshoe exists, Lebesgue almost all intial states may still converge to a stable steady state or to a stable cycle. On the other hand, in the numerical simulations in section 3 we have observed strange attractors for many parameter values. In this subsection we would like to refer to very recent results concerning the existence of strange attractors in two or higher dimensional models exhibiting a *homoclinic bifurcation* and discuss how these results can be applied to the addiction model. For an excellent mathematical treatment and a survey of the recent literature, we strongly recommend Palis and Takens [25].

Proving the existence of strange attractors in a model is a nontrivial task. For example, Hénon [14] presented numerical simulations suggesting a strange attractor in the by now well-known 2-D quadratic difference equation $(x_{n+1}, y_{n+1}) = (1 - ax_n^2 + y_n, by_n)$. However, it took 15 years before Benedicks and Carleson [3] finally were able to prove existence of strange, chaotic attractors for a large set (positive Lebesgue measure) of parameter values a and b in the Hénon-family. Their proof is long (about 100 pages) and complicated and there seems to be no easy way to directly "translate" the proof to a model like the present 2-D addiction model. Recently, Mora and Viana [24] have generalized this result proving the abundance of strange attractors (i.e. existence of strange attractors for a positive Lebesgue measure set of parameter values) in generic one-parameter families exhibiting a *homoclinic bifurcation*. A homoclinic orbit is an intersection point $q \neq p$ of the stable and unstable manifolds of a saddle point p (or of a periodic saddle point p). A homoclinic bifurcation is a bifurcation in which a homoclinic orbit is created or destroyed when a parameter changes.

The first economic applications of homoclinic bifurcation theory are the recent, very stimulating papers by de Vilder [32,33]. De Vilder presents elegant computer assisted proofs of homoclinic bifurcations in a 2-D version of the OLG-model with productive investment, implying existence of

strange attractors for large sets of parameter values even when the two consumption goods are gross substitutes. In another recent work, Brock and Hommes [4] prove the occurrence of homoclinic bifurcations and the associated dynamic complexities in a cobweb type demand-supply model with heterogeneous beliefs, where different groups of agents use different expectations functions, revising expectations over time based upon their past prediction performance.

Application of homoclinic bifurcation theory to 2-D economic models seems to be an important new step in analyzing economic fluctuations. We expect that the same methodology can also be applied in the 2-D addiction model. For example, varying the parameter γ we have the following. For small values of γ, say e.g. $\gamma = 0.5$, a globally stable steady state occurs. On the other hand, for large values of γ, e.g. for $\gamma = 3$, we have proven the existence of a horseshoe. It is well known that existence of a horseshoe implies existence of transversal homoclinic intersections. Therefore, there must be a bifurcation value $0.5 < \gamma_0 < 3$, at which a homoclinic bifurcation occurs. Applying the homoclinic bifurcation theory, under genericity assumptions (e.g. w.r.t. the consumption function), it follows that, for a large set of parameter values, strange attractors exist in the 2-D addiction model as well. This explains the strange attractors in our earlier numerical simulations. We will not pursue this issue in the present paper however; for details about homoclinic bifurcation theory and its applications in economics we refer the reader to the cited works.

5 Concluding remarks

We have investigated the consumption fluctuations in a simple, 2-D addiction model. The consumption patterns of addicted persons may be very erratic and seemingly unpredictable. We have shown the occurrence of topological chaos by locating a horseshoe, i.e. a chaotic invariant set, in some suitable rectangular region in the phase space. The erratic fluctuations are caused by a nonlinear feedback mechanism between the weight and consumption. When the parameter measuring the consumption elasticity w.r.t. weight is high this nonlinear feedback mechanism is strong and erratic fluctuations are likely to occur. Irregular consumption patterns can arise for a large set of parameter values.

Although in our model no optimization occurs, the model is related to the 'rational addiction' model by Becker and Murphy [2], in which addicted persons choose consumption according to utility optimization. To state it modestly, our model is at least not inconsistent with the rules suggested by an optimization framework. It remains to be seen whether an optimization framework can indeed yield behavioural rules leading to chaotic consumption fluctuations. This would be a useful topic for further research. In this respect we point out that our analysis can be carried out for a class of consumption feedback rules. The main geometric arguments for the existence of chaos rely on the shape of the consumption level curves.

Therefore, our analysis could be helpful in order to investigate which utility functions in an optimizing framework would yield behavioural rules leading to irregular consumption patterns.

In our model we have used discrete time. In [8] Dockner and Feichtinger have established the occurrence of limit cycles in a 2-D continuous time addiction model with optimization. Another interesting topic for further research would be to try to extend the Dockner-Feichtinger model to a 3-D system and investigate whether chaotic consumptions patterns can occur in continuous time.

A Proofs of the results

A.1 Proof of theorem 1

Fix $\beta = 0, \alpha = 0.1, \delta = \delta_0$ and $w_{min} = 10$. For $\beta = 0$ consumption $c(s,w) = 1/(w - w_{min})^{\gamma}$ only depends on w, so the consumption level curves are horizontal lines in the (s,w)-plane. The dynamics of w is, independently of s, described by a 1-D map f

$$w_{t+1} = (1-\alpha)w_t + \frac{1}{(w_t - w_{min})^{\gamma}} = f(w_t),$$

while

$$s_{t+1} = (1-\delta)s_t + \frac{1}{(w_t - w_{min})^{\gamma}}.$$

The derivative

$$f'(x) = 1 - \alpha - \frac{\gamma}{(x - w_{min})^{\gamma+1}}.$$

Let

$$x_{crit} = \left(\frac{\gamma}{1-\alpha}\right)^{1/(\gamma+1)} + w_{min}$$

be the critical point of the map 1-D f and write x^* for the fixed point of f. The map f is decreasing for $w_{min} < x < x_{crit}$, increasing for $x > x_{crit}$ and $f'(x) < 1 - \alpha$. For $\gamma = 0.25$ it can be checked that $f(x_{crit}) > x_{crit}$ implying that the fixed point x^* is globally stable.

Next assume that $\gamma \in [2.75, 50]$. First we prove that the 1-D map f has the following properties (see figure 7): there exists an interval $[\sigma, \tau]$ such that

1. $\sigma < x_{crit} < \tau$
2. f^3 is increasing on $[\sigma, x_{crit}]$ and decreasing on $[x_{crit}, \tau]$
3. $f^3(\sigma) < \sigma, f^3(\tau) < \tau$ and $f^3(x_{crit}) > \tau$

Properties 1–3 imply that the 1-D map f has infinitely many unstable periodic points and an uncountable set of aperiodic points. In order to prove

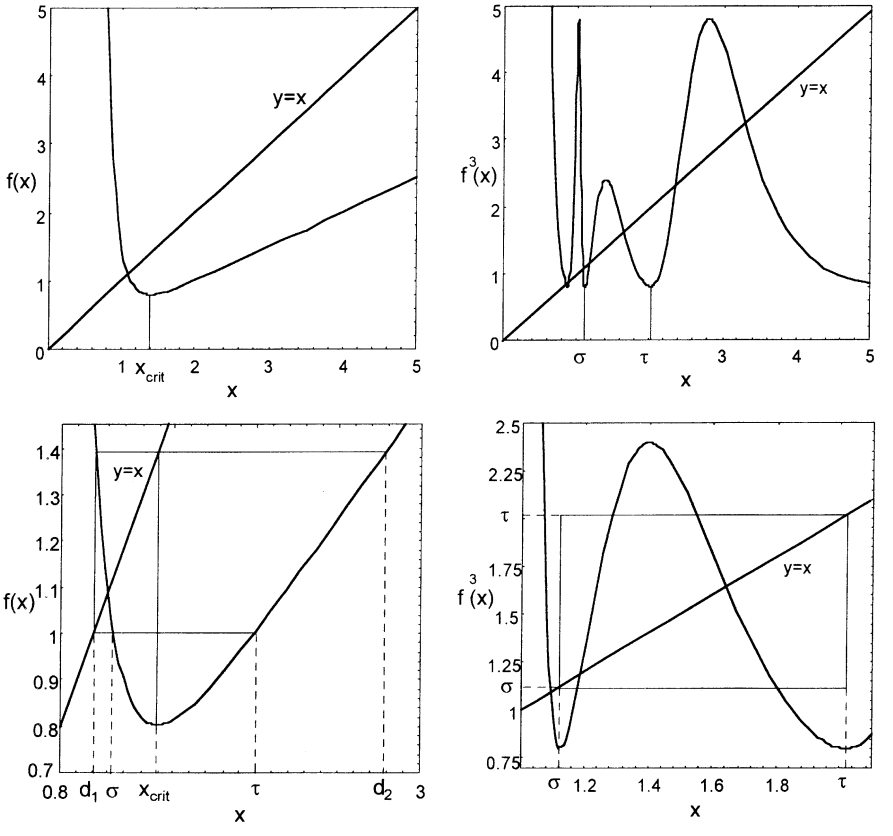

Figure 7a–d. $\alpha = \delta = 0.5, \beta = 0, \gamma = 3$. **a** Graph of the 1-D map $f(x) = (1-\alpha)x + 1/(x - w_{\min})^{\gamma}$. **b** Graph of the third iterate f^3. **(c)** Detail of the graph of f. The points $d_1 < \sigma < x_{crit} < \tau < d_2$, with $f(\sigma) = f(\tau) = d_1$ and $f(d_1) = f(d_2) = x_{crit}$, are indicated. **d** Detail of the graph of the third iterate f^3, with $f^3(\sigma) < \sigma, f^3(\tau) < \sigma$ and $f^3(x_{crit}) > \tau$.

properties 1–3, first note that

$$f(x_{crit}) = (1-\alpha)x_{crit} + \frac{1}{(x_{crit} - w_{min})^{\gamma}} = (1-\alpha)x_{crit} + \frac{(1-\alpha)(x_{crit} - w_{min})}{\gamma}$$

The following limits are easily obtained:

$$\lim_{\gamma \to \infty} x_{crit} = 1 + w_{min} \quad \text{and}$$

$$\lim_{\gamma \to \infty} f(x_{crit}) = (1-\alpha)(1 + w_{min})$$

From these limits it follows immediately that for γ large, $f(x_{crit}) < x_{crit}$ and the fixed point $x^* < x_{crit}$. Moreover, from the expression for the derivative $f'(x)$ it is clear that for γ large, the graph of f will be steep and

decreasing on the interval $[w_{min}, x_{crit}]$ and almost linear with slope $1-\alpha$ on the interval (x_{crit}, ∞). Let d_1 be the smallest and d_2 the largest inverse image of x_{crit}, i.e. $f(d_1) = f(d_2) = x_{crit}$, see figure 7c. For $\gamma \in [2.75, 50]$ d_1 has two inverse images σ and τ i.e. two points for which $f(\sigma) = f(\tau) = d_1$ or equivalently $f^2(\sigma) = f^2(\tau) = x_{crit}$. The points σ and τ are the critical points of f^3 which are closest to x_{crit}. The properties of the graph of f for γ large imply that $x^* < \sigma < x_{crit} < \tau < d_2 < f^3(x_{crit}) < f^2(x_{crit})$. Consequently, for $\gamma \in [2.75, 50]$ we have f^3 is increasing on $[\sigma, x_{crit}]$ and decreasing on $[x_{crit}, \tau]$, $f^3(\sigma) = f^3(\tau) = f(x_{crit}) < x^* < \sigma$ and $f^3(x_{crit}) > \tau$. This proves the properties 1–3 for $\gamma \in [2.75, 50]$[8].

Next we will show that the properties 1–3 for the 1-D map f imply that the third iterate F^3 of the 2-D map F has a horseshoe. From 1–3 it follows that there exist points $p_i, 1 \le i \le 4, \tau > p_1 > p_2 > x_{crit} > p_3 > p_4 > \sigma$ such that $f^3(p_1) = \sigma, f^3(p_2) = \tau, f^3(p_3) = \tau$ and $f^3(p_4) = \sigma$.

For $\beta = 0$ the consumption $c(s, w)$ is independent of s and we write $c(w)$. The weight w assumes values between $w_{min} = f(x_{crit})$ and $w_{max} = f^2(x_{crit})$, while consumption assumes values between $c_{min} = c(w_{max})$ and $c_{max} = c(w_{min})$. Let $s_{max} = c_{max}/\delta$, then $s_0 \le s_{max}$ implies $s_1 \le s_{max}$ and let $s_{min} = c_{min}$ then $s_0 \ge s_{min}$ implies $s_1 \ge s_{min}$. Consider the rectangular region $R = \overline{A_0 B_0 C_0 D_0}$, with

$$A_0 = (s_{min}, \tau) B_0 = (s_{max}, \tau)$$
$$C_0 = (s_{max}, \sigma) D_0 = (s_{min}, \sigma).$$

We claim that R contains a chaotic invariant set for F^3. Define the points

$$\begin{aligned} S_0 &= (s_{min}, p_1) & T_0 &= (s_{max}, p_1) \\ U_0 &= (s_{min}, p_2) & V_0 &= (s_{max}, p_2) \\ P_0 &= (s_{min}, x_{crit}) & Q_0 &= (s_{max}, x_{crit}), \\ W_0 &= (s_{min}, p_3) & X_0 &= (s_{max}, p_3) \\ Y_0 &= (s_{min}, p_4) & Z_0 &= (s_{max}, p_4) \end{aligned}$$

with $p_i, i = 1$ to 4, as defined before.

Recall that the 2-D map $F(s, w) = ((1-\delta)s + 1/(w - w_{min})^\gamma, (1-\alpha)w + 1/(w - w_{min})^\gamma)$. Since the second coordinate is independent of s, F maps horizontal line segments onto horizontal line segments, uniformly contracting them by a factor $1-\delta$ and then translating them over the vector $(1/(w - w_{min})^\gamma, (1-\alpha)w + 1/(w - w_{min})^\gamma)^T$, which only depends on w. In particular, any horizontal segment XY, with X lying left from Y, is mapped onto a horizontal segment $X'Y'$, with $X' = F(X)$ lying left from $Y' = F(Y)$. In the w-direction, the dynamics of F is completely determined by the 1-D map f. Using the properties 1–3 of the 1-D map f, it follows that $F(R), F^2(R)$ and $F^3(R)$ are as shown in figure 5. Writing $w(X)$ for the w-value of a point X, we have the following:

– in R: $w(A_0) = w(B_0) = \tau, w(P_0) = w(Q_0) = x_{crit}$ and $w(C_0) = w(D_0) = \sigma$.

[8] The problem for $\gamma > 50$, is that $f(x_{crit}) < x_{min}$ and the dynamics are undefined.

– in $F(R)$: $w(A_1) = w(B_1) = w(C_1) = w(D_1) = d_1$ and $w(P_1) = w(Q_1) = f(x_{crit})$.
– in $F^2(R)$: $w(A_2) = w(B_2) = w(C_2) = w(D_2) = x_{crit}$ and $w(P_2) = w(Q_2) = f^2(x_{crit})$.
– in $F^3(R)$: $w(A_3) = w(B_3) = w(C_3) = w(D_3) = f^3(\sigma) < \sigma$,
$w(S_3) = w(T_3) = w(Y_3) = w(Z_3) = \sigma$,
$w(U_3) = w(V_3) = w(W_3) = w(X_3) = \tau$, and
$w(P_3) = w(Q_3) = f^3(x_{crit}) > \tau$.

Hence, $F^3(R)$ has the form of a horseshoe folded over R.

Finally, we show that the region R contains a chaotic invariant set Λ of F^3 and we discuss the relation between the dynamics (under F^3) on Λ and the dynamics of the shift map on bi-infinite sequences of two symbols; we follow the approach in Palis and Takens [25 pp 22–28]. First we need some definitions. Define a *vertical strip* as a closed subset of R bounded in R by two disjoint continuous curves $\mathcal{L}_1$ and $\mathcal{L}_2$, without self intersections, connecting the sides A_0B_0 and C_0D_0. A *horizontal strip* is defined in an analogous way; see figure 8. F^3 is a 1-1 map from the horizontal strip $\mathcal{H}_0 = \overline{S_0T_0V_0U_0}$ to the vertical strip $\mathcal{V}_0 = \overline{S_3T_3V_3U_3}$ and from the horizontal strip $\mathcal{H}_1 = \overline{W_0X_0Z_0Y_0}$ to the vertical strip $\mathcal{V}_1 = \overline{W_3X_3Z_3Y_3}$; the horizontal strips $\overline{A_0B_0T_0S_0}$, $\overline{U_0V_0X_0W_0}$ and $\overline{Y_0Z_0C_0D_0}$ are mapped outside R.

We now make two additional assumptions:

– A1: the vertical strips $\mathcal{V}_0$ and $\mathcal{V}_1$ are disjoint (as in figure 5d).
– A2: the 1-D map f^3 is expanding (i.e. $|(f^3)'(x)| \geq \mu > 1$) on the intervals $[p_1, p_2]$ and $[p_3, p_4]$.

Assumption A1 will be satisfied when the contraction factor $1 - \delta$ in the horizontal direction is sufficiently small. We checked numerically that assumption A2 is satisfied for $\gamma \in [2.75, 50]$. Below we discuss what happens when these two assumptions are not satisfied.

Let $(Z_2)^Z$ be the set of bi-infinite sequences of two symbols 0 and 1. So an element $z \in (Z_2)^Z$ is $z = (\ldots z_{-3}z_{-2}z_{-1}.z_0z_1z_2\ldots)$, where $z_i = 0$ or $z_i = 1$. The shift map σ: $(Z_2)^Z \to (Z_2)^Z$ is defined as $\sigma(z) = (\ldots z_{-3}z_{-2}z_{-1}z_0.z_1z_2\ldots)$.

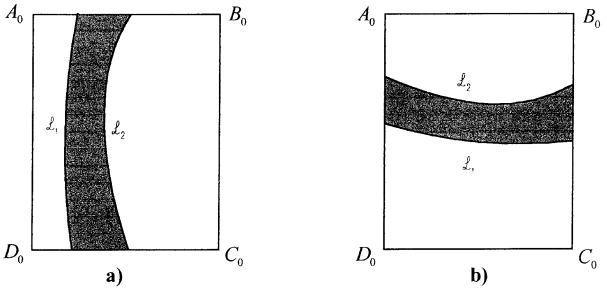

Figure 8. **a** vertical strips, **b** horizontal strips.

We claim that the dynamics of F^3 on the maximal invariant set $\Lambda \in R$ is topologically conjugate to the shift map on bi-infinite sequences:

Claim 1. *Under assumptions A1 and A2, the maximal invariant set $\Lambda \in R$ (under F^3) is a Lebesgue-measure zero Cantor set. There exists a homeomorphism $h : \Lambda \to (Z_2)^Z$, such that $h(X) = z = (\ldots z_{-3}z_{-2}z_{-1}.z_0z_1z_2\ldots)$ with $F^{3i}(X) \in \mathcal{V}_0$ when $z_i = 0$ and $F^{3i}(X) \in \mathcal{V}_1$ when $z_i = 1$ for all $i \in Z$. Moreover, h preserves the dynamics, i.e. $\sigma \circ h = h \circ F^3$.*

The proof of the claim follows by first constructing a nested sequence of horizontal strips in essentially the same way as for Smale's classical horseshoe. Write G for the map F^3. Each horizontal strip $\mathcal{H}_i, i = 0, 1$ contains two smaller horizontal strips of points X for which $G^k(X) \in \mathcal{V}_0 \cup \mathcal{V}_1, k = 0, 1$ or 2. Continuing in the same way, there exist 2^n disjoint horizontal strips consisting of points X for which $G^k(X) \in \mathcal{V}_0 \cup \mathcal{V}_1$ for $0 \leq k \leq n$. From assumption A2 it follows that the total height of the 2^n vertical strips is smaller than $(1/\mu)^n$ times the height of R. Hence, the forward invariant set L^+ is a zero Lebesgue measure Cantor set of horizontal line segments. In the same way, using assumption A1 it can be shown that the backward invariant set L^-, that is, the set of points X for which $G^{-n}(X) \in R$ for all $n \in \mathcal{N}$, is a zero Lebesgue measure Cantor set of vertical curve segments. The maximal invariant set in R is given by $\Lambda = L^+ \cap L^-$. The set of points that remain in R for both positive and negative time is thus an intersection of Cantor sets of vertical and horizontal curve segments. This proves the claim.

When assumption A1 is not satisfied the backward invariant set L^- need not be a Cantor set of vertical curves. For example, when the two vertical strips $\mathcal{V}_0$ and $\mathcal{V}_1$ coincide, the set L^- may even consist of one single vertical curve. The forward invariant set is a Cantor set of horizontal line segments however, as long as assumption A2 is satisfied. When A2 does not hold, the forward invariant set can be a larger set, and the construction above only implies that L^+ contains a Cantor set of horizontal line segments. In the latter case, the same construction can be used to show that the invariant set Λ contains a smaller set Λ^* where the dynamics is topologically conjugate to the shift map on one-sided infinite sequences of two symbols 0 and 1.

We conclude that for $\gamma \in [2.75, 50]$, also when A1 and A2 are not satisfied, the map F^3 has a chaotic invariant set $\Lambda \in R$. Consequently, $\Lambda \cup F(\Lambda) \cup F^2(\Lambda)$ is a chaotic invariant set of F. This completes the proof of theorem 1.

A.2 Proof of theorem 2

The 2-D map $F(s, w) = ((1 - \delta)s + c(s, w), (1 - \alpha)w + c(s, w))$, with consumption $c(s, w) = s^\beta/(w - w_{min})^\gamma$, has a simple structure: it consists of a linear contraction with factor $(1 - \delta)$ in the s- and factor $(1 - \alpha)$ in the w-direction followed by a translation over the consumption vector $(c(s, w),$

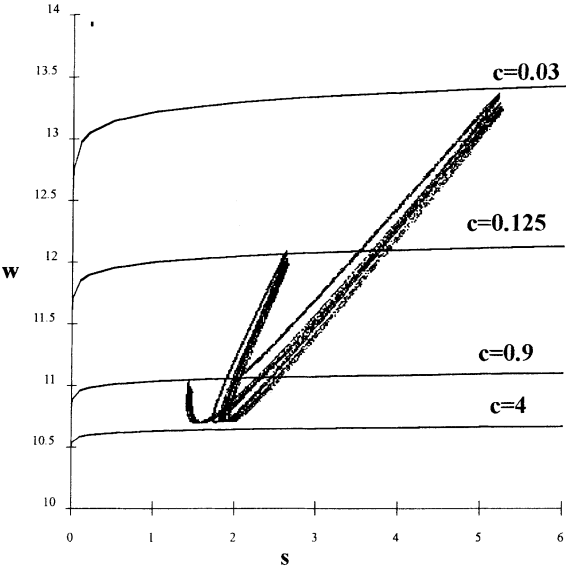

Figure 9. $\alpha = 0.1, \beta = 0.1, \gamma = 3, \delta = 0.5$ and $w_{min} = 10$. The strange, chaotic attractor with some consumption levelcurves $c(s, w) = constant$.

$c(s, w)$) in the diagonal direction. The length of the translation vector depends on the point (s, w). In order to understand the global dynamics the levelcurves of consumption $c(s, w)$ in the (s, w)-phase space play an important role. For γ large these level curves have the property that they are almost vertical when s is close to zero, while they are almost horizontal for s-values not close too zero, cf. figure 9. In that case, unless s is close to zero, the level of consumption is in fact determined by w only. For large w-values consumption is close to zero: only for smaller w-values consumption assumes larger positive values.

The previous *geometric* arguments play a crucial role in understanding the occurrence of chaos. We will work them out in detail in the benchmark case, but we emphasize that the same arguments are valid for a large set of parameter values and even for different expressions of the consumption $c(s, w)$ with level curves having similar shapes.

Fix $\alpha = 0.1, \beta = 0.1, \gamma = 3$ and $w_{min} = 10$. First consider the case $\delta = 0.5$. Let R_1 be the rectangular region $R_1 = \overline{A_0 B_0 C_0 D_0}$ with $A_0 = (3.8, 13)$, $B_0 = (4.3, 13)$, $C_0 = (3.4, 12.1)$ and $D_0 = (2.9, 12.1)$. For a point $X_0 = (s, w)$ we write $X_i = F^i(X_0), i \in N$, and $c(X_0)$ for the corresponding consumption $c(s, w)$. R_1 consists of horizontal line segments, and each of these horizontal line segment is close to one levelcurve of consumption. We have $c(A_0) \approx c(B_0) \approx 0.0002$ and $c(C_0) \approx c(D_0) \approx 0.0044$, so for points in R_1 the translation is almost zero and F almost acts as a linear contraction. The corner points of the region $F(R_1)$ and their corresponding consump-

tions are (in 3 decimals accuracy):

$$\begin{array}{ll} A_1 \approx (1.125, 1.913) & c(A_1) \approx 0.021 \\ B_1 \approx (1.275, 1.914) & c(B_1) \approx 0.021 \\ C_1 \approx (0.754, 1.129) & c(C_1) \approx 0.468 \\ D_1 \approx (0.604, 1.129) & c(D_1) \approx 0.458 \end{array}$$

$\overline{A_1B_1}$ and $\overline{C_1D_1}$ are still approximately horizontal line segments, each of them having approximately the same consumption. While the consumption corresponding to the segment $\overline{A_1B_1}$ is small (about 0.02) the consumption corresponding to $\overline{C_1D_1}$ is larger (about 0.46). Recall that F is a contraction followed by a translation. For the upper part of $F(R_1)$ the translation vector is close to zero, while for the lower part the translation vector is larger (about 0.46 in both the s- and the w-direction). In fact $F^2(R_1)$ is obtained from $F(R_1)$ by a linear contraction followed by a folding, see figure 6b. The folding occurs approximately along the 'segment' $\overline{P_2Q_2}$, where $P_2 \approx (1.289, 10.644)$ and $Q_2 \approx (1.419, 10.650)$, with consumptions $c(P_2) \approx 3.837$ and $c(Q_2) \approx 3.774$. The corresponding original points P_0 and Q_0 in R_1 are $P_0 \approx (3.35, 12.55)$ and $Q_0 \approx (3.85, 12.55)$. The values of P_0 and Q_0 have numerically been obtained by looking for that horizontal line segment $\overline{X_0Y_0}$ in R_1 for which the w-value of X_2 (and Y_2) was minimal, or equivalently (since the consumption level curves are close to horizontal lines in that part of the phase space) for which the consumption $c(X_2) \approx c(Y_2)$ is maximal. The corner points of the region $F^2(R_1)$ and their corresponding consumptions are:

$$\begin{array}{ll} A_2 \approx (0.358, 0.881) & c(A_2) \approx 1.925 \\ B_2 \approx (0.404, 0.882) & c(B_2) \approx 1.945 \\ P_2 \approx (1.289, 10.644) & c(P_2) \approx 3.837 \\ Q_2 \approx (1.419, 10.650) & c(Q_2) \approx 3.774 \\ C_2 \approx (0.695, 0.977) & c(C_2) \approx 1.112 \\ D_2 \approx (0.640, 0.966) & c(D_2) \approx 1.174 \end{array}$$

The consumption corresponding to points in $F^2(R_1)$ is so large that the translation dominates the linear contraction, so that $F^3(R_1)$ will be further away from the origin, see figure 6b. The endpoints of $F^3(R_1)$ are:

$$\begin{array}{ll} A_3 \approx (2.033, 2.322) & c(A_3) \approx 0.007 \\ B_3 \approx (2.066, 2.341) & c(B_3) \approx 0.007 \\ P_3 \approx (4.864, 5.099) & c(P_3) \approx 0.000 \\ Q_3 \approx (4.866, 5.087) & c(Q_3) \approx 0.000 \\ C_3 \approx (1.320, 1.551) & c(C_3) \approx 0.074 \\ D_3 \approx (1.366, 1.609) & c(D_3) \approx 0.060 \end{array}$$

In fact $F^3(R_1)$ is mapped like a 'horseshoe' over R_1 (see figure 10). With the same definitions of horizontal and vertical strips as in the proof of theorem 1, we have: F^3 maps the horizontal strip $H_0 = \overline{S_0T_0V_0U_0}$ onto the vertical strip $V_0 = \overline{S_3T_3V_3U_3}$, the horizontal strip $H_1 = \overline{W_0X_0Z_0Y_0}$ onto the vertical

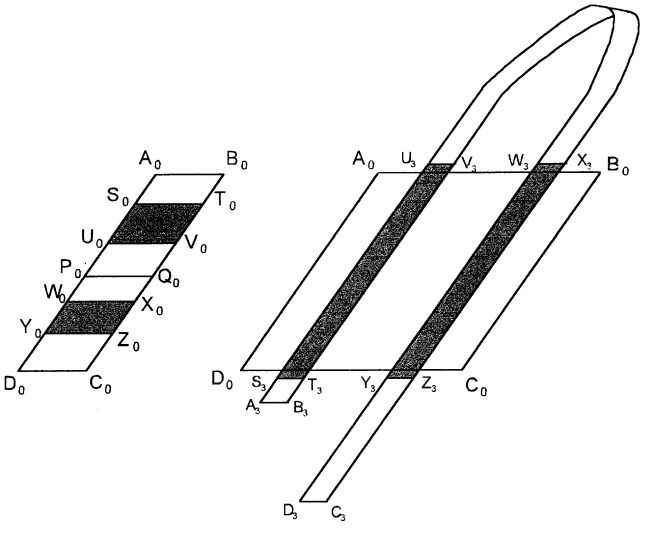

Figure 10. The third iterate F^3 maps the rectangular region $R_1 = \overline{A_0B_0C_0D_0}$ in the form of a horseshoe over itself.

strip $V_1 = \overline{W_3X_3Z_3Y_3}$ and the horizontal strips $\overline{A_0B_0T_0T_0S_0}$, $\overline{U_0V_0X_0W_0}$ and $\overline{Y_0Z_0C_0D_0}$ outside the region R_1, where

$$\begin{array}{llll} S_0 = (3.76, 12.96) & T_0 = (4.26, 12.96) & S_3 \approx (2.983, 12.071) & T_3 \approx (3.044, 12.071) \\ U_0 = (3.5, 12.7) & V_0 = (4, 12.7) & U_3 \approx (4.145, 13.127) & V_3 \approx (4.175, 13.096) \\ W_0 = (3.22, 12.42) & X_0 = (3.72, 12.42) & W_3 \approx (4.249, 13.157) & X_3 \approx (4.237, 13.085) \\ Y_0 = (3.04, 12.24) & Z_0 = (3.54, 12.24) & Y_3 \approx (3.165, 12.066) & Z_3 \approx (3.166, 12.009). \end{array}$$

From a topological viewpoint, the situation is now exactly the same as for the horseshoe in the proof of theorem 1 (see figure 5). By the same construction as in the proof of theorem 1, it therefore follows that the region R_1 contains a chaotic invariant set Λ.

Finally, consider the case $\delta = 0.2$. The same construction can be applied. The only difference is that the vertical strips $\mathcal{V}_0$ and $\mathcal{V}_1$ are not disjoint, but overlap. From the proof of theorem 1 it follows however that in this case R_2 also contains a chaotic invariant set. This completes the proof of theorem 2.

References

1. Becker, G.S.: Habits, addictions and traditions. Kyklos **45**, 327–346 (1992)
2. Becker, G.S., Murphy, K.M.: A theory of rational addiction. Journal of Political Economy **96**, 675–700 (1988)
3. Benedicks, M., Carleson,L.: The dynamics of the Hénon-map. Annals of Mathematics **133**, 73–169 (1991)
4. Brock, W.A., Hommes, C.H.:Rational routes to randomness. Department of Economics, University of Wisconsin, RM9506, 1995

5. Brock, W.A., Hsieh, D.A., LeBaron, B.: Nonlinear dynamics, chaos and instability. Statistical theory and economic evidence. Cambridge, Massachusetts: MIT Press 1991
6. Day, R.H.: Complex economic dynamics, vol I + II. MIT Press, 1995
7. Dvaney, R.L.: An introduction to chaotic dynamical systems, 2nd edition. Redwood City: Addison-Wesley 1989
8. Dockner, E.J., Feichtinger, G.: Cyclical consumption patterns and rational addiction. American Economic Review **83**, 256–263 (1993)
9. Feichtinger, G.: Rational addictive cycles ('binges') under a budget constraint. Optimal Control Applications and Methods **13**, 95–104 (1992)
10. Feichtinger, G.: Strange addictive behaviour: periodic and chaotic binges. In: Mathematical modelling in economics: essays in honor of Wolfhang Eichhorn. Diewert, W.E., Spremann, K., Stehling, F. (eds.) Heidelberg, New York: pp. 149–162 Berlin, Springer, 1993
11. Feichtinger, G., Hartl, R.F., Sethi, S.P.: Dynamic optimal models in advertising: recent developments. Management Science (1994)
12. Feichtinger, G., Wirl, F.: Complex addictive consumption paths – nonlinear modifications of a model of Becker and Murphy. Working Paper, Technical University, Vienna (1993)
13. Gulick, D.: Encounters with chaos. McGraw-Hill, New York, 1992
14. Hénon, M.: A two-dimensional mapping with a strange attractor. Communications in Mathematical Physics **50**, 69–77 (1976)
15. Hicks, J.R.: Capital and growth. Oxford: Clarendon Press, 1965
16. Hommes, C.H.: Chaotic dynamics in economic models: some simple casestudies. Groningen Theses in Economics, Management & Organization. Groningen: Wolters-Noordhoff 1991
17. Iannaccone, L.R.: Addiction and satiation. Economics Letters **21**, 95–99 (1986)
18. Léonard, D.: Market behaviour of rational addicts. Journal of Economic Psychology **10**, 117–144 (1989)
19. Li, T.-Y., Yorke, J.A.: Period three implies chaos. American Mathematical Monthly **82**, 985–992 (1975)
20. Lorenz, H.-W.: Nonlinear dynamical economics and chaotic motion. In: Lecture Notes in Economics and Mathematical Systems 334, 2nd revised and enlarged edition. Berlin, Heidelberg, New York: Springer 1993
21. Majumdar, M: Some remarks on optimal growth with intertemporally dependent preferences in the neoclassical model. Review of Economic Studies **42**, 147–53 (1975)
22. Medio, A.: Chaotic dynamics. Theory and applications to economics. Cambridge: Cambridge University Press 1992
23. Milnor, J.: On the concept of attractor. Communications in Mathematical Physics **99**, 177–195 (1985)
24. Mora, L., Viana, M.: Abundance of strange attractors. Acta Mathematica **171**, 1–71 (1993)
25. Palis, J., Takens, F.: Hyperbolicity and sensitive chaotic dynamics at homoclinic bifurcations. Cambridge: Cambridge University Press 1993
26. Ryder Jr., H.E., Heal, G.M.: Optimal growth with intertemporally dependent preferences. Review of Economic Studies **40**, 1–33 (1973)
27. Samuelson, P.A.: Turnpike theorems even though tastes are intertemporally dependent. Western Economic Journal **9**, 21–26 (1971)
28. Smale, S.: Diffeomorphisms with many periodic points. In: Cairns S.S (ed.) Differential and combinatorial topology. Princeton: Princeton University Press 1965
29. Sorger, G.: Chaotic Ramsey equilibrium. International Journal of Bifurcations and Chaos **5**, 373–380 (1995)
30. Spitzer, F., Wan, H.: The characterization of optimal saving programs in a quadratic model. Journal of Mathematical Economics **3**, 43–79 (1976)

31. Stigler, G.J., Becker, G.S.: De gustibus non est disputandum. American Economic Review **67**, 76–90 (1977)
32. de Vilder, R.G.: Complicated endogenous business cycles under gross substitutability. CNRS/CEPREMAP working paper No 9501. Journal of Economic Theory, forthcoming (1995)
33. de Vilder, R.G.: Endogenous business cycles. Tinbergen Institute Research Series 96, Ph-D thesis University of Amsterdam, 1995
34. Wan, H.Y.: Optimal saving programs under intertemporally dependent preferences. International Economic Review **11**, 521–547 (1970)